

Supplementary Information

Experimental

Synthesis of 1

Nickel(II) acetate tetrahydrate (1 mmol $\text{Ni}(\text{C}_2\text{H}_3\text{O}_2)_2 \cdot 4\text{H}_2\text{O}$, 0.2488 g) was dissolved in 20 cm³ water and combined with 2,6-dimethanolpyridine (2 mmol, 0.2783 g) in 10 cm³ of water. Resulting mixture was stirred for few min; then 3,5-dinitrobenzoic acid (2 mmol, 0.4242 g) in 10 cm³ of water was added and resulting mixture was stirred for 2 hours. After filtration it was left for crystallization under ambient temperature. Light pink-red crystals suitable for X-Ray data collection were collected after four days. Yield 0.18 g. Elemental analysis for $[\text{Ni}(\text{pydm})_2](\text{dnbz})_2$; found: N 10.96, C 43.93, H 3.13, calc.: N 11.07, C 44.30, H 3.19 %.

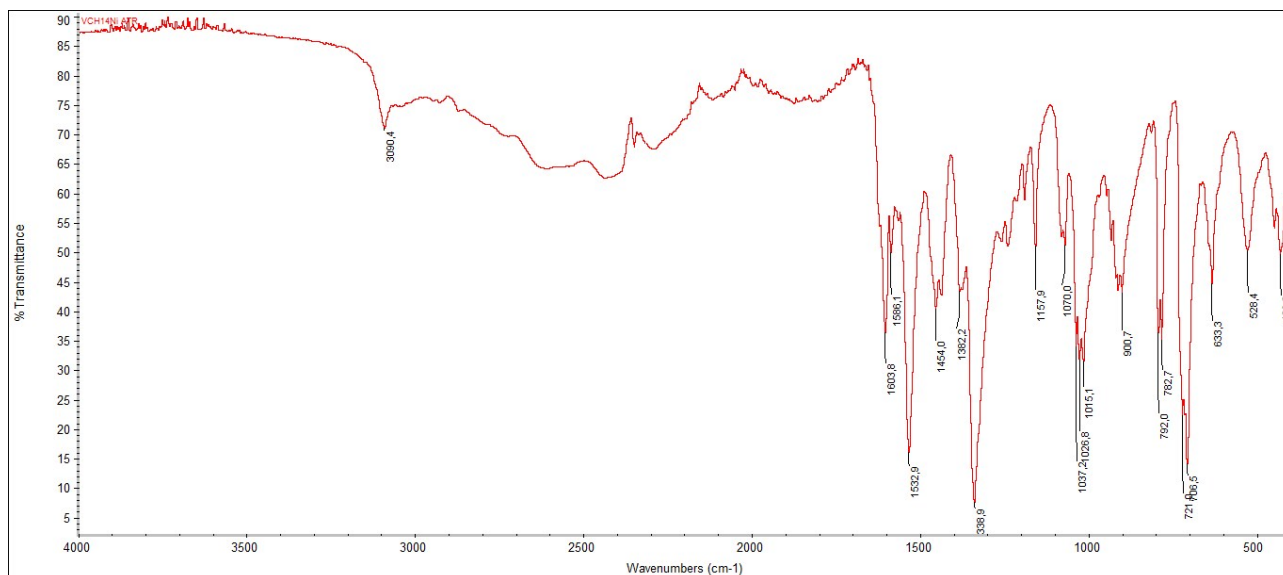


Figure S1. IR spectrum of 1

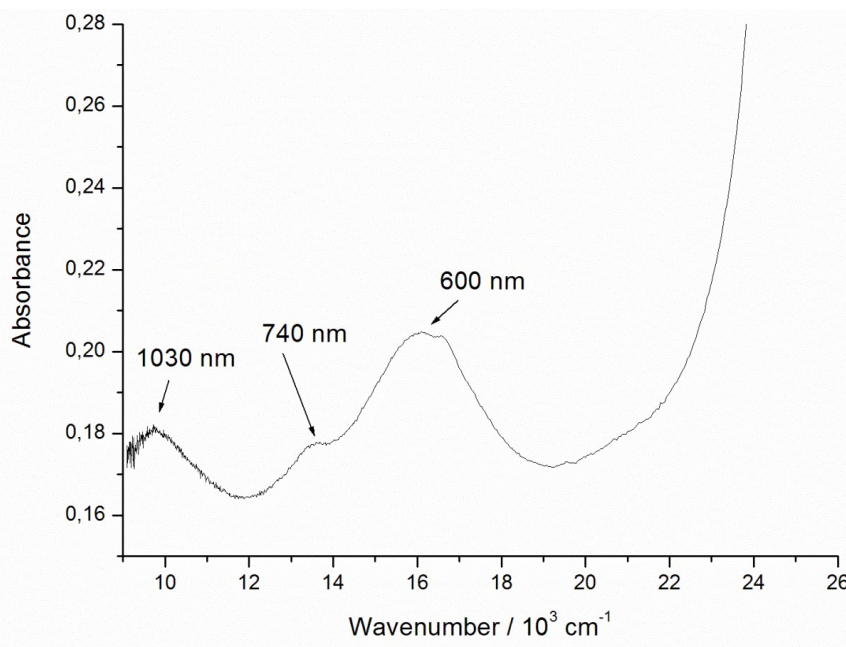


Figure S2. Electronic spectrum of 1.

X-ray structure determination

Table S1. Crystal data and results of refinement for **1**.

| | |
|---|--|
| Empirical formula | C ₂₈ H ₂₄ N ₆ NiO ₁₆ |
| Formula weight [g mol ⁻¹] | 759.24 |
| Crystal system, space group | Triclinic, <i>P</i> −1 |
| Unit cell dimensions [Å, deg, Å ³] | <i>a</i> = 7.9708(2) <i>b</i> = 13.7985(4) <i>c</i> = 14.6800(4) α = 96.452(2) β = 103.366(2) γ = 100.715(2) <i>V</i> = 1522.94(7) |
| <i>Z</i> | 2 |
| Calculated density [Mg m ⁻³] | 1.656 |
| Absorption coefficient [mm ⁻¹] | 1.733 |
| Crystal form, colour, size [mm] | green, block 0.22 × 0.12 × 0.08 |
| Temperature [K] | 100(1) |
| Radiation [Å] | 1.54186 |
| Diffractometer | Stoe StadiVari |
| θ range for data collection [°] | 6.272 to 142.306 |
| Index ranges | -9 ≤ <i>h</i> ≤ 6, -15 ≤ <i>k</i> ≤ 16, -18 ≤ <i>l</i> ≤ 16 |
| Reflections coll. / indep. / parameters. | 25529 / 5722 / 461 |
| GooF (S) all/ind. | 1.052 |
| Final <i>R</i> indices [<i>I</i> > 2σ(<i>I</i>)] | R ₁ = 0.0308, wR ₂ = 0.0799 |
| <i>R</i> indices (all data) | R ₁ = 0.0316, wR ₂ = 0.0805 |
| Largest diff. peak and hole [e Å ⁻³] | 0.45 / -0.34 |

Table S2. Selected geometric parameters [Å, deg] for **1**.

| | | | |
|-----------|------------|-----------|------------|
| Ni1–N1 | 1.9808(12) | Ni1–N2 | 1.9798(12) |
| Ni1–O1 | 2.0856(11) | Ni1–O2 | 2.0924(11) |
| Ni1–O3 | 2.1356(11) | Ni1–O4 | 2.1301(11) |
| O1–Co1–O2 | 157.73(4) | O1–Co1–O3 | 95.37(4) |
| O1–Co1–O4 | 89.28(4) | O2–Co1–O3 | 91.93(4) |
| O2–Co1–O4 | 91.92(4) | O3–Co1–O4 | 157.66(4) |
| N1–Co1–O1 | 79.27(5) | N1–Co1–O2 | 79.37(5) |
| N1–Co1–O3 | 92.94(5) | N1–Co1–O4 | 109.40(5) |
| N2–Co1–O1 | 99.91(5) | N2–Co1–O2 | 102.13(5) |
| N2–Co1–O3 | 78.82(5) | N2–Co1–O4 | 78.85(5) |
| N1–Co1–N2 | 171.64(5) | | |

Table S3. Possible hydrogen bonds (Å, °) for **1**.

| D–H···A | d(D–H) | d(H···A) | d(D···A) | <(DHA) |
|------------------------------|--------|----------|----------|--------|
| O1–H1···O11 | 0.86 | 1.68 | 2.536(2) | 169 |
| O2–H2···O6 | 0.87 | 1.69 | 2.558(2) | 175 |
| O3–H3···O12 | 0.87 | 1.75 | 2.602(2) | 163 |
| O4–H4···O5 | 0.987 | 1.75 | 2.580(2) | 160 |
| C1–H1B···O16 ⁱ | 0.99 | 2.39 | 3.194(2) | 138 |
| C7–H7A···O11 ⁱⁱⁱ | 0.99 | 2.37 | 3.320(2) | 160 |
| C11–H11···O11 ⁱⁱ | 0.95 | 2.60 | 3.292(2) | 130 |
| C28–H28···O14 ⁱⁱⁱ | 0.95 | 2.46 | 3.247(2) | 141 |

Symmetry code: (i) -x, -y, -z; (ii) 1-x, 1-y, 1-z; (iii) 1+x, y, z.

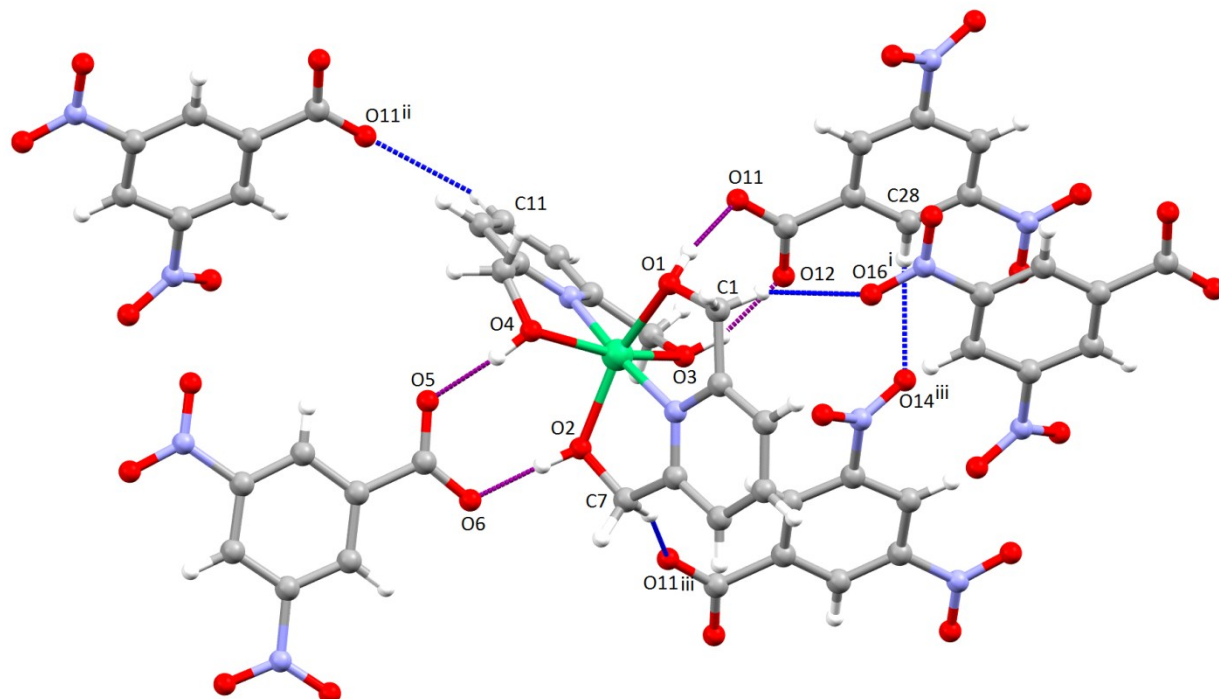


Figure S3. View of the O–H···O (violet dashes lines) and C–H···O (blue dashes lines) hydrogen bonding system in **1**.

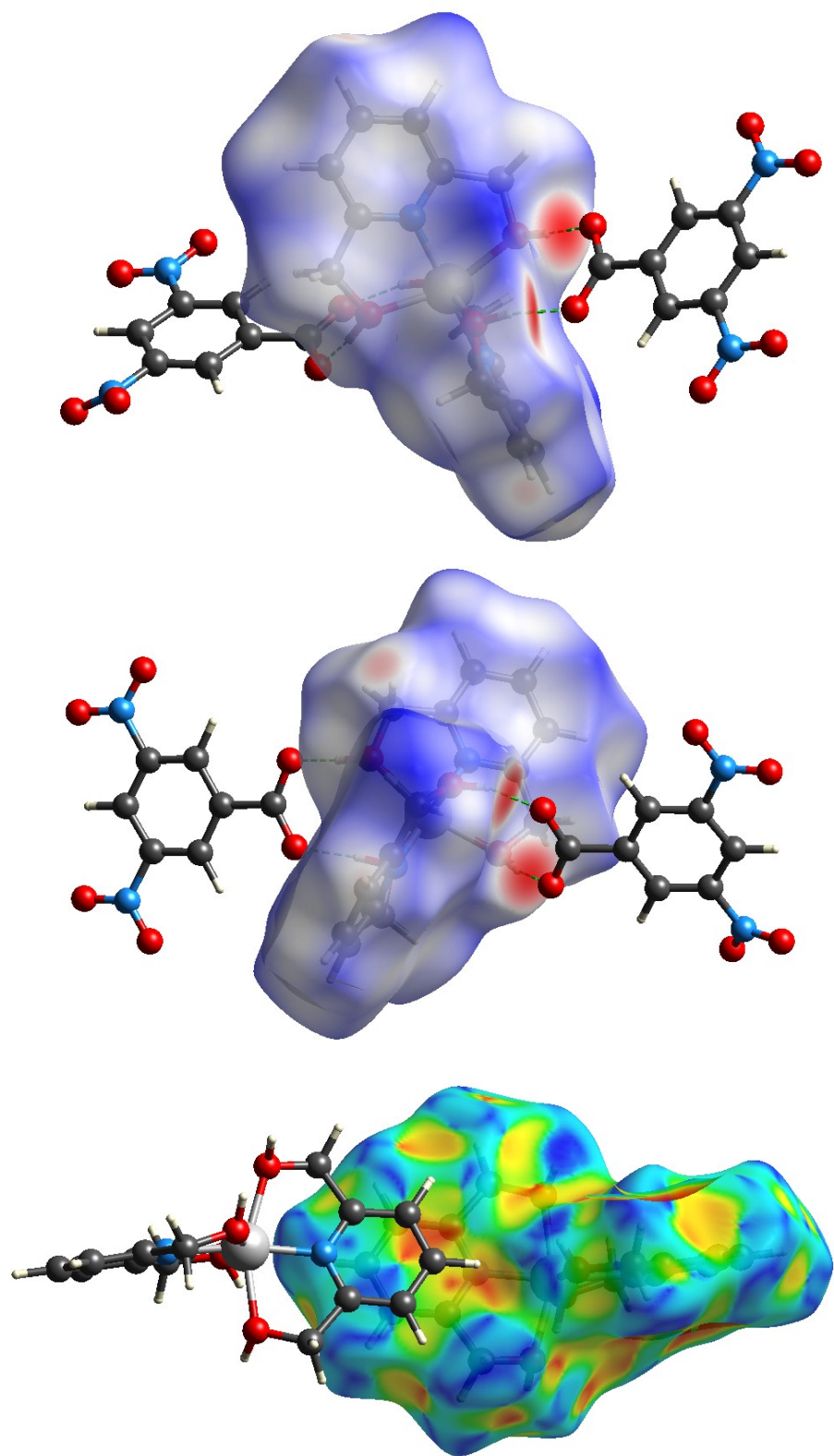


Figure S4. View of the three-dimensional Hirshfeld surface of **1** plotted over d_{norm} in the range -0.8134 to 0.4339 a. u. (top) and shape-index with indications of π - π stacking interactions (bottom).

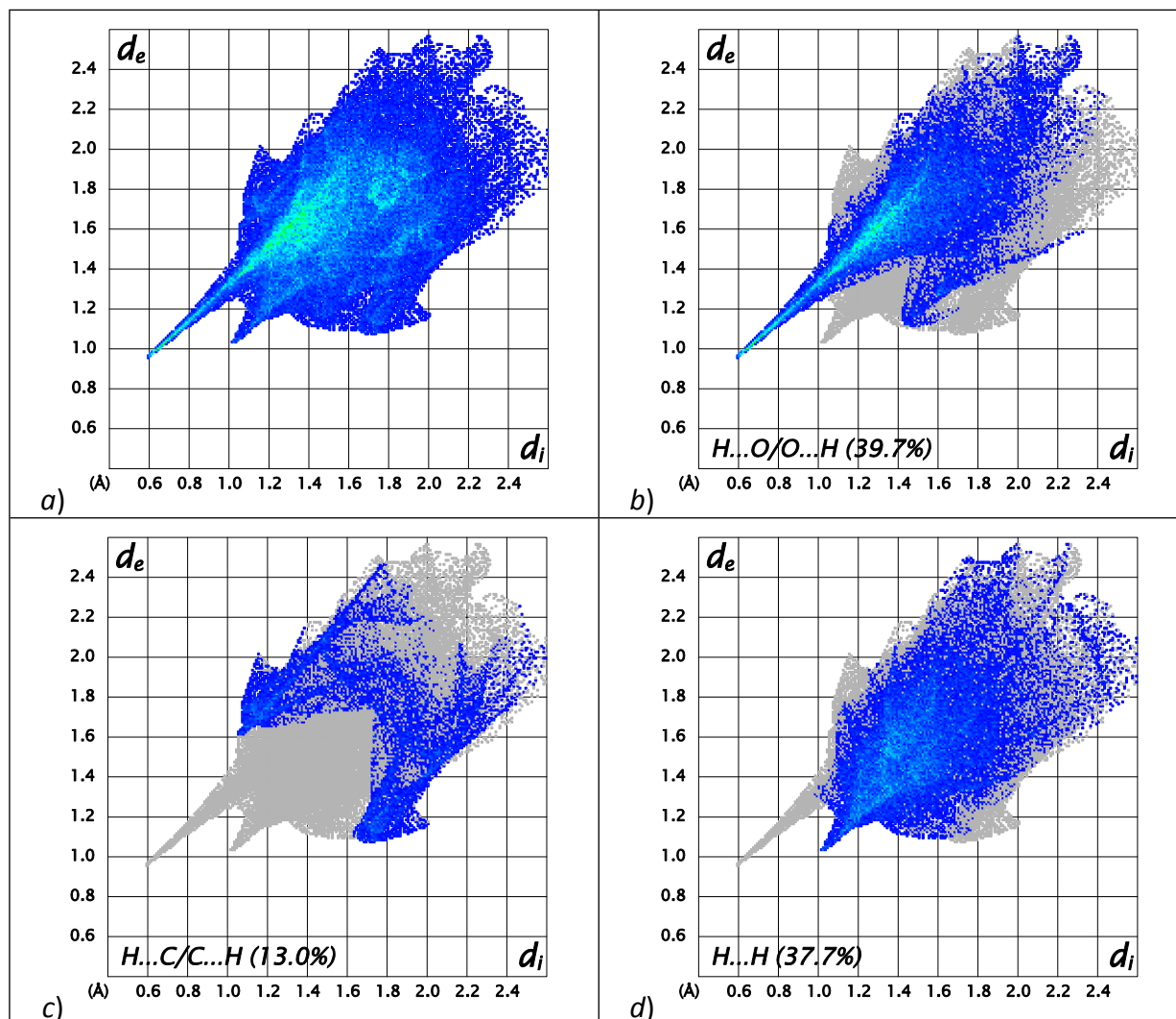


Figure S5. The full two-dimensional fingerprint plots of **1**, showing (a) all interactions, and delineated into (b) $H\cdots O/O\cdots H$, (c) $H\cdots C/C\cdots H$ and (d) $H\cdots H$ interactions. The d_i and d_e values are the closest internal and external distances from given on the Hirshfeld surface contacts.

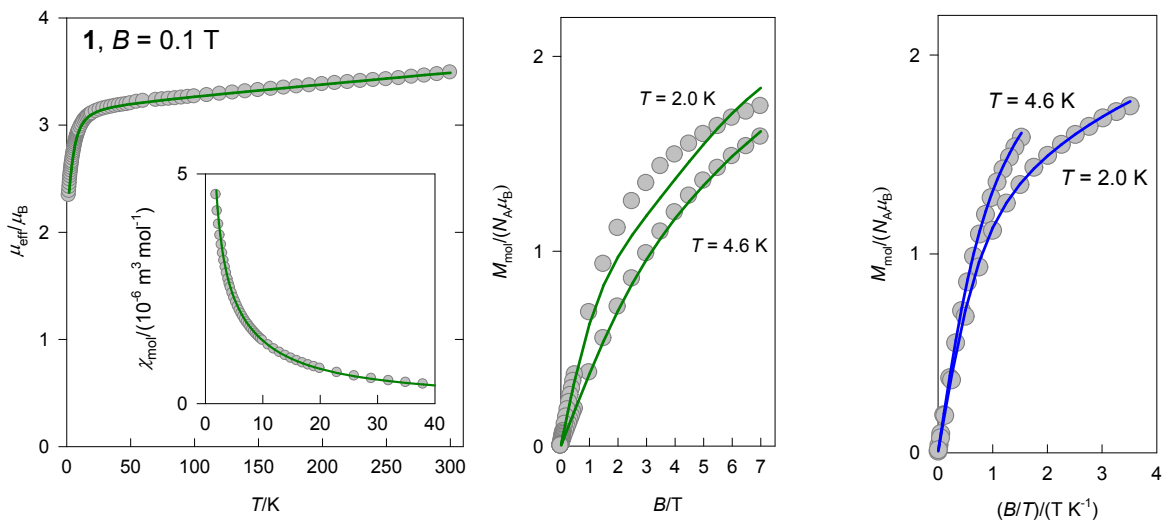


Figure S6. Alternative fit of DC magnetic data for **1** using the zero-field splitting model: $g_{\text{iso}} = 2.230$, $D/hc = -12.63 \text{ cm}^{-1}$, $\chi_{\text{TIM}} = 11.63 \times 10^{-9} \text{ m}^3 \text{ mol}^{-1}$, $zj/hc = -0.05 \text{ cm}^{-1}$; $R(\chi) = 0.0026$, $R(M) = 0.036$. Right – reduced magnetization with the preferred model described in the main text.

***Ab initio* calculations**

Ab initio calculations were performed with ORCA 4.0.0 computational package using the experimental geometry of complex under study. The relativistic effects were included in the calculations with zero-order regular approximation (ZORA) together with the scalar relativistic contracted version of def2-TZVPP basis functions for Ni atom and def2-SV(P) basis functions for other elements. The calculations of ZFS parameters were based on state average complete active space self-consistent field (SA-CASSCF) wave functions complemented by N-electron valence second order perturbation theory (NEVPT2). The active space of the CASSCF calculations comprised of eight electrons in five metal-based d-orbitals. The state averaged approach was used, in which all 10 triplet and 15 singlet states were equally weighted. The calculations utilized the RI approximation with appropriate decontracted auxiliary basis set and the chain-of-spheres (RIJCOSX) approximation to exact exchange. Increased integration grids (Grid4 and GridX5) and tight SCF convergence criteria were used. The ZFS parameters were calculated through quasi-degenerate perturbation theory in which an approximation to the Breit-Pauli form of the spin-orbit coupling operator (SOMF) and the effective Hamiltonian theory was utilized.

Table S4. Calculated CAS(8,5)/NEVPT2 transition energies and their contributions to *D* and *E* parameters for **1**.

| Root | Multiplicity | E_i/cm^{-1} | D_i/cm^{-1} | E_i/cm^{-1} |
|------|--------------|----------------------|----------------------|----------------------|
| 0 | 3 | 0 | | |
| 1 | 3 | 7258 | -57.59 | 0.19 |
| 2 | 3 | 9769 | 19.64 | -19.31 |
| 3 | 3 | 10820 | 16.64 | 16.84 |
| 4 | 3 | 16181 | 1.12 | 0.99 |
| 5 | 3 | 16933 | 0.9 | -0.9 |
| 6 | 3 | 18193 | 0.21 | 0.22 |
| 7 | 3 | 26620 | 0.07 | 0.05 |
| 8 | 3 | 27199 | 0.06 | -0.05 |
| 9 | 3 | 29842 | 0 | 0 |
| | | | | |
| 0 | 1 | 13458 | -0.02 | 0.02 |
| 1 | 1 | 16171 | 0 | 0 |
| 2 | 1 | 23080 | 16.16 | -0.01 |
| 3 | 1 | 24731 | -6.32 | 5.7 |
| 4 | 1 | 25721 | -5.9 | -5.15 |
| 5 | 1 | 29302 | -0.01 | 0.02 |
| 6 | 1 | 30404 | -0.62 | -0.66 |
| 7 | 1 | 30929 | -0.56 | 0.53 |
| 8 | 1 | 35341 | -0.04 | -0.05 |
| 9 | 1 | 37463 | 0 | 0 |
| 10 | 1 | 37696 | 1.3 | -0.01 |
| 11 | 1 | 39070 | -0.27 | -0.04 |
| 12 | 1 | 39154 | -0.69 | -0.26 |
| 13 | 1 | 39573 | -0.86 | 0.23 |
| 14 | 1 | 67132 | 0 | 0 |

Dominant contributions are **bold** typed.

Spin-orbit splitting of the ground term: $\Delta E^{\text{SOC}} = 0, 2.9, 16.1 \text{ cm}^{-1}$.

AC susceptibility data

A three set Debye model of the relaxation is based upon the equation

$$\chi(\omega) = \chi_s + \sum_{k=1}^3 \frac{\chi_{T_k} - \chi_s}{1 + (i\omega\tau_k)^{1-\alpha_k}}$$

containing up to 10 free parameters: the isothermal susceptibilities χ_{T_k} , the distribution parameters α_k and the relaxation times τ_k for each relaxation channel, along with the adiabatic susceptibility χ_s . The above equation can be decomposed into the real and imaginary components, e.g.

$$\begin{aligned}\chi'(\omega) &= \chi_s + (\chi_{T_1} - \chi_s) \frac{1 + (\omega\tau_1)^{1-\alpha_1} \sin(\pi\alpha_1/2)}{1 + 2(\omega\tau_1)^{1-\alpha_1} \sin(\pi\alpha_1/2) + (\omega\tau_1)^{2-2\alpha_1}} \\ &\quad + (\chi_{T_2} - \chi_{T_1}) \frac{1 + (\omega\tau_2)^{1-\alpha_2} \sin(\pi\alpha_2/2)}{1 + 2(\omega\tau_2)^{1-\alpha_2} \sin(\pi\alpha_2/2) + (\omega\tau_2)^{2-2\alpha_2}} + \dots \\ \chi''(\omega) &= (\chi_{T_1} - \chi_s) \frac{(\omega\tau_1)^{1-\alpha_1} \cos(\pi\alpha_1/2)}{1 + 2(\omega\tau_1)^{1-\alpha_1} \sin(\pi\alpha_1/2) + (\omega\tau_1)^{2-2\alpha_1}} \\ &\quad + (\chi_{T_2} - \chi_{T_1}) \frac{(\omega\tau_2)^{1-\alpha_2} \cos(\pi\alpha_2/2)}{1 + 2(\omega\tau_2)^{1-\alpha_2} \sin(\pi\alpha_2/2) + (\omega\tau_2)^{2-2\alpha_2}} + \dots\end{aligned}$$

that are fitted simultaneously by minimizing a joint functional formed of the weighted sum of the relative errors

$$F = w \cdot E(\chi') + (1-w) \cdot E(\chi'')$$

with

$$E(\chi) = \sum_i^n \frac{|\chi_i^o - \chi_i^c|}{\chi_i^o}$$

Table S5. Field dependence of AC susceptibility parameters for **1** at $T = 1.9$ K.^a

| B_{DC}/T | $R(\chi')$ % | $R(\chi'')$ % | χ_s | χ_{LF} | α_{LF} | τ_{LF} / s | χ_{IF} | α_{IF} | τ_{IF} /10 ⁻³ s | χ_{HF} | α_{HF} | τ_{HF} /10 ⁻⁶ s | x_{LF} | x_{IF} | x_{HF} |
|------------|-----------------|------------------|----------|-------------|---------------|--------------------|-------------|---------------|------------------------------------|-------------|---------------|------------------------------------|----------|----------|----------|
| 0.2 | 0.31 | 22 | 5.2(1) | 5.3(1) | .00 | 0.82(35) | - | - | - | 5.45(2) | .11(9) | 599 | .30 | - | .70 |
| 0.4 | 0.22 | 7.6 | 4.5(2) | 4.7(2) | .04 | 1.05(12) | 4.9(5) | .04 | 0.29(11) | 5.28(3) | .51(12) | 798 | .33 | .21 | .46 |
| 0.6 | 0.46 | 6.0 | 3.7(2) | 4.3(2) | .17 | 1.29(24) | 4.4(7) | .00 | 0.27(40) | 5.05(8) | .48(16) | 398 | .45 | .05 | .50 |
| 0.8 | 0.63 | 4.5 | 3.2(1) | 3.8(1) | .00 | 1.30(14) | 3.9(1) | .00 | 83(51) | 4.57(8) | .42(9) | 503 | .47 | .07 | .46 |
| 1.0 | 3.4 | 6.8 | 2.7(2) | 3.4(4) | .00 | 1.22(43) | 3.5(3) | .03 | 82 | 4.01(12) | .34 | 536 | .52 | .10 | .38 |

^a Obtained by a three-set Debye model; χ in units of 10⁻⁶ m³ mol⁻¹.

$x_{LF} = (\chi_{T,LF} - \chi_s)/(\chi_T - \chi_s)$, $x_{IF} = (\chi_{T,IF} - \chi_{T,LF})/(\chi_T - \chi_s)$, $x_{HF} = (\chi_{T,HF} - \chi_{T,IF})/(\chi_T - \chi_s)$, $\chi_{T,HF} = \chi_T$.

Table S6. Results of the fitting procedure for AC susceptibility components of **1** at $B_{DC} = 0.6$ T.^a

| T/K | $R(\chi')$ % | $R(\chi'')$ % | χ_s | χ_{LF} | α_{LF} | τ_{LF} / s | χ_{HF} | α_{HF} | τ_{HF} /10 ⁻⁶ s | x_{LF} |
|-------|-----------------|------------------|----------|-------------|---------------|--------------------|-------------|---------------|------------------------------------|----------|
| 1.9 | 0.57 | 6.6 | 3.7(1) | 4.2(1) | .15(5) | 0.72(7) | 5.0(1) | .38(5) | 255(53) | .39 |
| 2.1 | 0.66 | 9.2 | 3.6(1) | 4.1(1) | .19(6) | 0.66(8) | 4.7(3) | .35(7) | 225(63) | .43 |
| 2.3 | 0.64 | 6.4 | 3.4(1) | 3.8(1) | .15(6) | 0.64(7) | 4.5(1) | .45(7) | 131(69) | .37 |
| 2.5 | 1.1 | 9.5 | 3.4(2) | 3.8(2) | .21(12) | 0.55(13) | 4.3(1) | .40(17) | 159(139) | .43 |
| 2.7 | 0.68 | 11 | 3.4(1) | 3.8(1) | .20(8) | 0.49(7) | 4.1(1) | .30(13) | 210(104) | .53 |
| 2.9 | 0.94 | 16 | 3.3(1) | 3.6(1) | .12(11) | 0.48(9) | 3.9(1) | .30(15) | 407(170) | .51 |
| 3.1 | 0.66 | 20 | 3.3(1) | 3.6(1) | .22(10) | 0.47(11) | 3.7(1) | .15(17) | 345(109) | .63 |
| 3.5 | 0.96 | 12 | 3.1(1) | 3.3(1) | .09(13) | 0.43(9) | 3.4(1) | .08(23) | 511(210) | .63 |
| 3.9 | 1.3 | 19 | 3.0(1) | 3.1(1) | .07(24) | 0.47(18) | 3.2(1) | .01(35) | 653(343) | .62 |
| 4.3 | 0.36 | 16 | 2.8(1) | 2.9(1) | .16(10) | 0.59(12) | 2.9(1) | .03(19) | 687(215) | .68 |

^a Obtained by a two-set Debye model; χ in units of 10⁻⁶ m³ mol⁻¹.

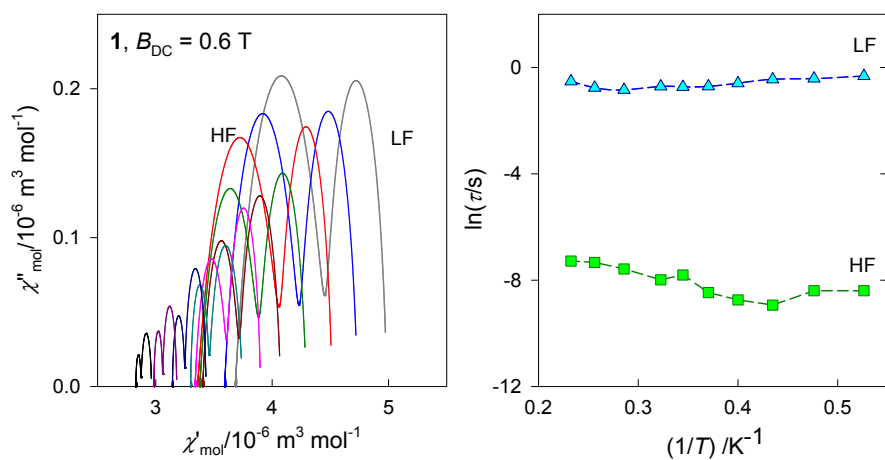


Figure S7. Fitted AC susceptibility data for **1**: Argand diagram (left) formed of two overlapping arcs, and Arrhenius-like plot (right).

Table S7. Comparison of AC and DC magnetic parameters for Ni(II) SIMs.

| Complex | B_{DC}/T | T/K | τ/s | U/cm^{-1} | $(D/hc)/\text{cm}^{-1}$ | Ref. |
|--|--------------------------|--------------|---|--------------------|-------------------------|-----------|
| 1 | 0.8 | 1.9 | 1.30 (LF) 5.03×10^{-8} (HF) | n.a. | -15.4 | This work |
| Ni(<i>pydc</i>)(<i>pydm</i>)·H ₂ O | 0.2 | 2.1 | 0.077 (LF) 3.83×10^{-7} (HF)* | 14.7 | -13.7 | [1] |
| [Ni(NCS) ₂ (<i>nqu</i>) ₂ (H ₂ O) ₂]·2 <i>nqu</i> | 0.4 | 1.9 | 0.275 (LF) | n.a. | -5.86 | [2] |
| [Ni(<i>mdabco</i>) ₂ Cl ₃]ClO ₄ | 0.2 | 2.0 | 5.3×10^{-5} (HF) 3.1×10^{-8} * | 19.3 | -311 | [3] |

* τ_0 values extracted from Arrhenius equation fit.

(1) J. Miklovič, D. Valigura, R. Boča and J. Titiš, *Dalton Trans.*, 2015, **44**, 12484.

(2) D. Lomjanský, J. Moncoľ, C. Rajnák, J. Titiš and R. Boča, *Chem. Commun.*, 2017, **53**, 6930.

(3) K. E. R. Marriott, L. Bhaskaran, C. Wilson, M. Medarde, S. T. Ochsenbein, S. Hill and M. Murrie, *Chem. Sci.*, 2015, **6**, 6823.

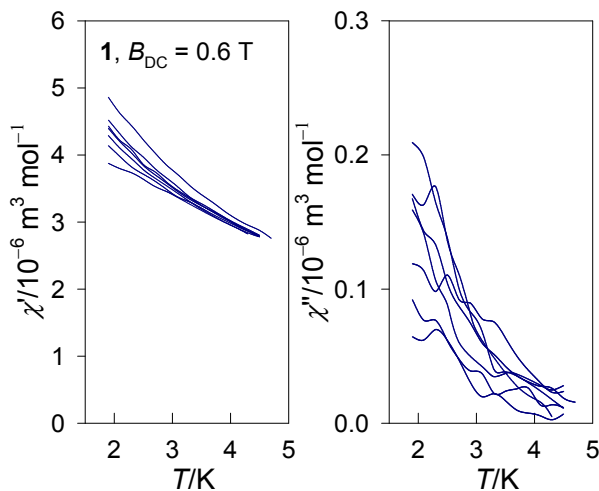


Figure S8. Temperature dependence of the AC susceptibility components for 1 at $B_{\text{DC}} = 0.6 \text{ T}$ for a set of frequencies $f = 0.1, 1.0, 10, 40, 158, 629$, and 1488 Hz .